Supplementary Materials:

Materials and Methods

Strain construction

For a listing of strains used in figures, see Table S1. All strains are derivatives of *B. subtilis* 168 *trpC2* unless otherwise noted. For additional details of strain and plasmid construction, see Tables S2 and S3, respectively.

Media and culture conditions

B. subtilis cultures were grown in the chemically defined minimal medium S7 (1), modified from (2), supplemented with trace elements (3) and L-tryptophan to early log phase. For all experiments shown, cells were grown to early log phase, OD_{600} ~0.1-0.2. Dilutions for OD_{600} matching, if required, were no more than 1:3.

Microscopy & image analysis

Microscopy was performed on live cells immobilized on 1% agarose pads prepared with S7 media. Imaging was performed using a Nikon 90i or a TE2000 microscope with a 100x Phase contrast objective (CFI Plan Apo Lambda DM 100x Oil, NA 1.45), an X-Cite light source, a Hamamatsu Orca ER-AG, and the following filter cubes: YFP (ET Sputter 500/20x, Dm515, 535/30m), and mCherry (ET Sputter Ex560/40 Dm585 Em630/75). To generate representative fields of log phase cultures, cultures were concentrated ~20-100x immediately prior to imaging. Images were processed using Fiji(4).

Quantitative measurement of gene expression was performed similarly to (5). Briefly, phase contrast and fluorescence images (e.g., YFP, mCherry) were acquired of well separated bacterial cells immobilized on agarose pads. The resulting image stacks were segmented based on the phase contrast image, and the corresponding average florescence per pixel within each cell was

calculated for each fluorescence channel using Matlab. A non-fluorescent control strain, treated with antibiotics as needed, was used as a control to subtract background and autofluorescence in each channel.

Luminescence assays

Luminescence assays were performed as described (6) with the following modifications. The cultures were initially grown to early log phase in a roller drum at 37ºC. 150 µl of each culture was then loaded into each well and 100 µg/ml bacitracin was added as indicated. Luminescence and OD_{600} were measured at 5 min intervals and the values of all samples at a defined time point after the luminescence reached ~steady state, about 1h post treatment, are reported.

Flow cytometry and cell sorting

Cultures were grown to early log phase and diluted 2-4 fold with additional S7 media to obtain the optimal density for flow cytometry. The resulting samples were vortexed vigorously prior to measurement to disrupt aggregates. Flow cytometry and sorting were performed on a BD Biosciences FACS Aria II-SORP. YFP was detected using a blue laser (488 nm) with a 525/50 dichroic, and a 505 long pass filter. mCherry was detected using a yellow/green laser (561 nm) with a 582/15 dichroic, and a 570 long pass filter. Fluorescence values were quantitatively compared between experiments by rescaling each experiment by the mean fluorescence of a control sample. Sorting was performed with a 70 nm nozzle at 70 PSI. Detection voltages were set such that the non-fluorescent control had a median value of ~100.

Survival assays

$1.5*10^4$ cells were sorted by fluorescence, and dispensed into equal volumes of chemically defined growth media (S7). Cultures were incubated in a roller drum at 37ºC for 10 min, then treated with 500 ng/ml ciprofloxacin for 3.5h. Serial dilutions of each population were plated for colony forming units (CFUs) on LB and grown overnight at 30ºC and survival ratios were

calculated by comparing the CFU values between the high and low fluorescence groups. In each experiment, wild-type and mutant strains were tested in parallel.

Autofluorescence deconvolution method and validation

For each flow cytometry experiment, data from both *sasA* reporter strains and a non-fluorescent control were measured. Raw measurements of fluorescence intensities from transcriptional reporter strains have two contributions: (i) the transcriptional reporter for *sasA* expression (e.g. P_{sasA}-*yfp*), the signal of interest; and (ii) background fluorescence originating from other sources. Measuring the statistics of the background fluorescence using a non-fluorescent control allowed extraction (deconvolution) of the *sasA* transcriptional reporter signal from the total raw measurement consisting of the sum of this signal and background fluorescence (7). This was done by calculating the mean and variance of the measured raw fluorescence signal from reporter strains, and, separately, the background fluorescence signal measured using the non-fluorescent control. Numerical estimates for the statistics of the signal of interest from the *sasA* transcriptional reporter were then obtained by assuming that this signal is not correlated with background fluorescence. (This assumption is supported by fluorescence microscopy experiments showing that cell size was not well correlated with *sasA* expression, and by computationally verifying that simple forms of dependency are inconsistent with the observed data.) The mean and variance of fluorescence from the *sasA* transcriptional reporter could then be uniquely determined, as described in more detail in the mathematical details of the deconvolution procedure. We used a Gamma distribution to model the distribution of the fluorescence signal for a given mean and variance. The Gamma distribution is routinely applied to fit gene expression data (8), but here we additionally verified that it closely mimics the underlying signal coming from the reporter by an *in-silico* re-convolution of the Gamma-distribution-fitted autofluorescence-free signal with measured background fluorescence. The resulting total fluorescence statistics closely resemble those that

were originally measured (Fig. S3). We separately verified that other distribution choices, such as lognormal, did not capture the data as well.

Mathematical details of deconvolution procedure

The raw fluorescence intensity (R) measured from transcriptional reporter strains were assumed to have two statistically independent contributions. One coming from the signal of interest (S), and one coming from other sources, collectively treated here as noise (N). One then has

$$R = S + N ,$$

for every measurement taken, and averaging over all measurements immediately gives the following relation

$$< R >= < S > + < N >$$

between the mean fluorescence values of the raw fluorescence intensity, the signal of interest, and the noise. Statistical independence then asserts that the variance in the fluorescence intensity could also be decomposed in a similar way

$$Var(R) = Var(S) + Var(N) .$$

These relations, and the fact $< R >$, $< N >$, $Var(R)$, $Var(N)$ could all be directly computed from measured data allowed us to estimate the mean, $< S >$,and variance, $Var(S)$, of the signal of interest. The full distribution of the signal of interest was then assumed to be well described by a Gamma distribution, since this has previously been shown to correctly describe gene expression data in bacteria (8) and we have moreover verified that this assumption is internally consistent with the data (materials and methods). The probability density function describing S was therefore modeled as

$$f(s) = \frac{1}{\Gamma(k)\theta^k} s^{k-1} e^{-s/\theta},$$

where $\Gamma(\cdot)$ denotes the gamma function, and the parameters k and θ are uniquely set by their relations to the mean

$$< S > = k\theta,$$

and variance

$$Var(S) = k\theta^2,$$

of the signal.

Mathematical details of enrichment model

Deconvolved fluorescence intensities of cells before, $f_b(s)$, and after, $f_a(s)$, ciprofloxacin treatment were modeled by the Gamma distribution to test the hypothesis that they are related via

$$f_a(s) = C \cdot f_b(s) \cdot p(s)\,,$$

where $p(s)$ stands for the probability of a cell with fluorescence intensity s to survive the prescribed treatment and C is a normalization constant assuring that

$$\int_0^\infty f_a(s)ds = \int_0^\infty C \cdot f_b(s) \cdot p(s)ds = 1\,.$$

Following treatment, we define the enrichment factor (in the probability density) of cells with fluorescence level s as

$$EF(s) = f_a(s)/f_b(s)\,.$$

One could then write the ratio between the survival probability of cells with fluorescence s_1 and s_2 (Survival Ratio) in the following way

$$\text{Survival Ratio} = \frac{p(s_1)}{p(s_2)} = \frac{C \cdot p(s_1)}{C \cdot p(s_2)} = \frac{f_a(s_1)/f_b(s_1)}{f_a(s_2)/f_b(s_2)}.$$

This relation was then used to predict survival ratios and compare with data as described in the main text.

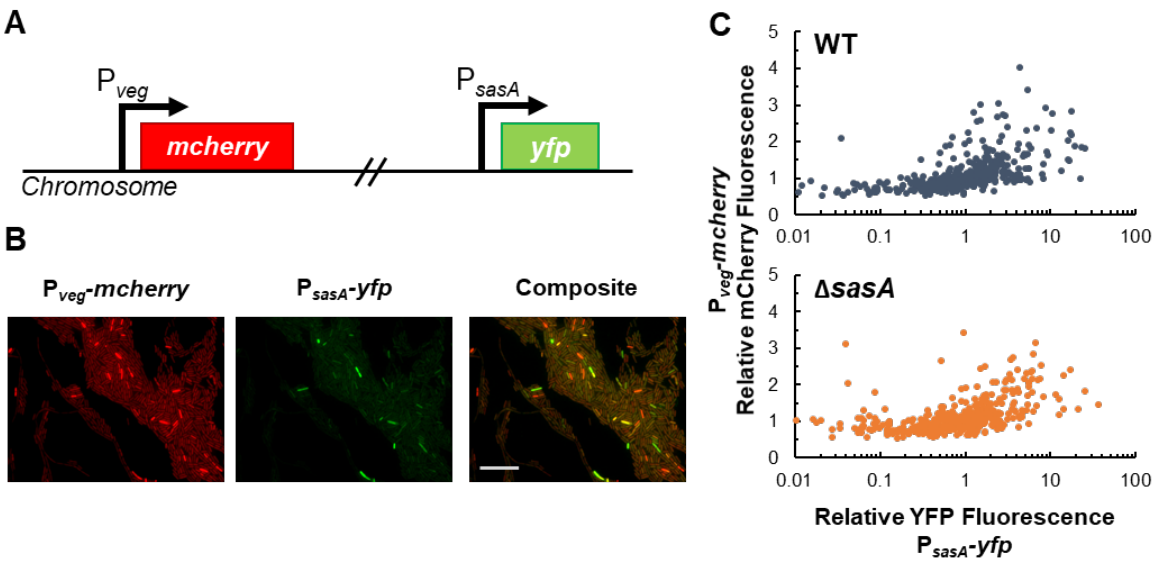

Figure S1: Comparison of P_{sasA}-*yfp* and the constitutive reporter P_{veg}-*mcherry*

A) Schematic of dual-color transcriptional reporter strain used to measure the correlation in the expression of *sasA* and *veg*. Two transcriptional reporters, P_{veg}-*mcherry* and P_{sasA}-*yfp* are inserted at ectopic loci.

B) Correlation of P_{veg} and P_{sasA} activity in single cells. Individual fluorescence channels and a composite image of a dual reporter strain P_{sasA}-*yfp* P_{veg}-*mcherry* in log phase growth. **Left:** P_{veg}-*mcherry* reporter displays cell-to-cell variability. **Center:** P_{sasA}-*yfp* reporter in the same population displays cell-to-cell variability. **Right:** Composite image with mCherry and YFP images. Scale bar indicates 10 μm.

C) Quantification of the correlation between P_{sasA}-*yfp* and P_{veg}-*mcherry* expression in single cells in an otherwise WT (**top**) or a Δ*sasA* (**bottom**) background. Cellular fluorescence intensities were measured for single cells described in **(A,B)** in 4 experiments (at least 540 cells). Relative fluorescence is the fluorescence of each individual cell relative to the mean fluorescence of the population in each channel and is plotted on a linear scale (mCherry) or a log scale (YFP). The Pearson's correlation coefficients of the relative

136 fluorescence values are WT: r ~ 0.50 ± 0.0084, Δ*sasA*: r ~ 0.52 ± 0.099 (mean ± SEM, 4
137 experiments).
138

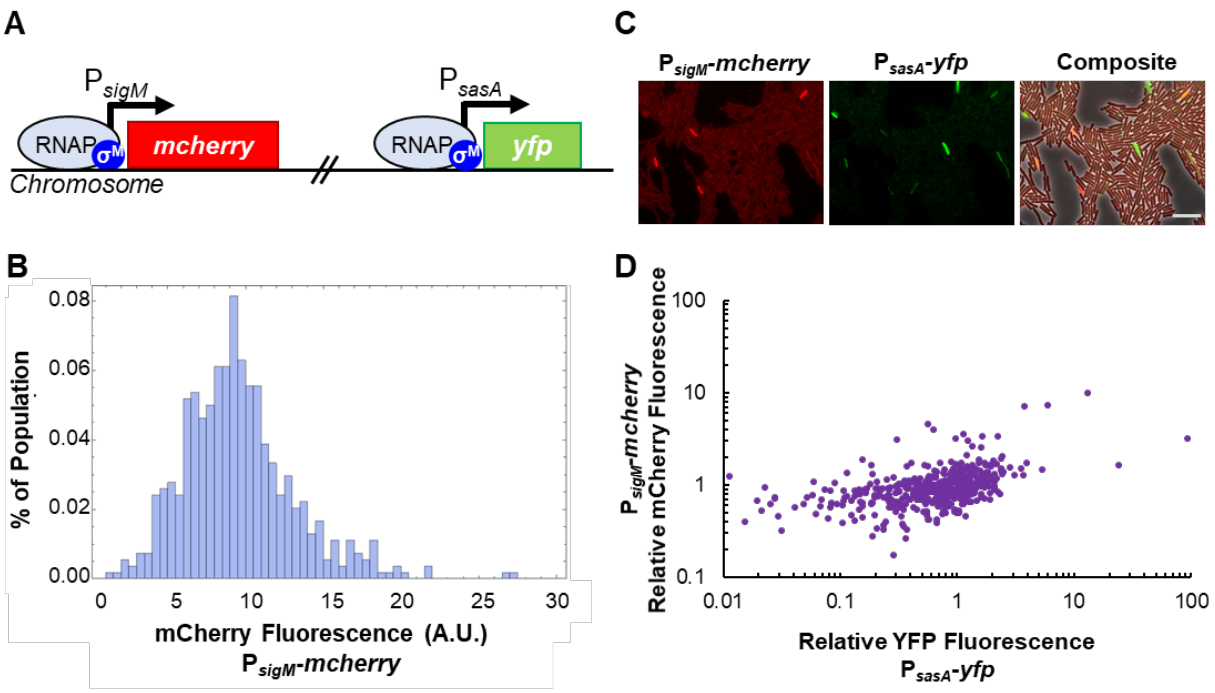

Figure S2: Correlation of cell-to-cell variability in *sigM* and *sasA*

A) Schematic of dual-color transcriptional reporter strain used to measure the correlation in the expression in *sasA* and *sigM*. Two transcriptional reporters, P_{sigM}-*mcherry* and P_{sasA}-*yfp,* are inserted at ectopic loci. Both *sigM* and *sasA* transcription use the alternative sigma factor σ^M (SigM) of RNAP.

B) Quantification of the distribution of P_{sigM}-*mcherry* expression in a log phase culture in the absence of a specific inducing stress. Histogram of the mCherry fluorescence intensities per cell, background subtracted, for ~540 individual cells. The CV ~ 0.77 ± 0.098 (SEM, 3 experiments).

C) Correlation of P_{sigM} and P_{sasA} activity in single cells. Fluorescence and composite phase contrast images of the dual reporter strain P_{sasA}-*yfp* P_{sigM}-*mcherry* in log phase growth. **Left:** P_{sigM}-*mcherry* reporter displays cell-to-cell variability. **Center:** P_{sasA}-*yfp* reporter in the same population displays cell-to-cell variability. **Right:** Composite image with phase contrast, mCherry, and YFP images. Scale bar indicates 10 μm.

D) Quantification of the correlation between P_{sasA}-*yfp* and P_{sigM}-*mcherry* expression in single cells. Cellular fluorescence intensities were measured for single cells described in (**A,C)**. The Pearson's correlation coefficient of the relative fluorescence values is r ~ 0.35 ± 0.087 (SEM, 3 experiments).

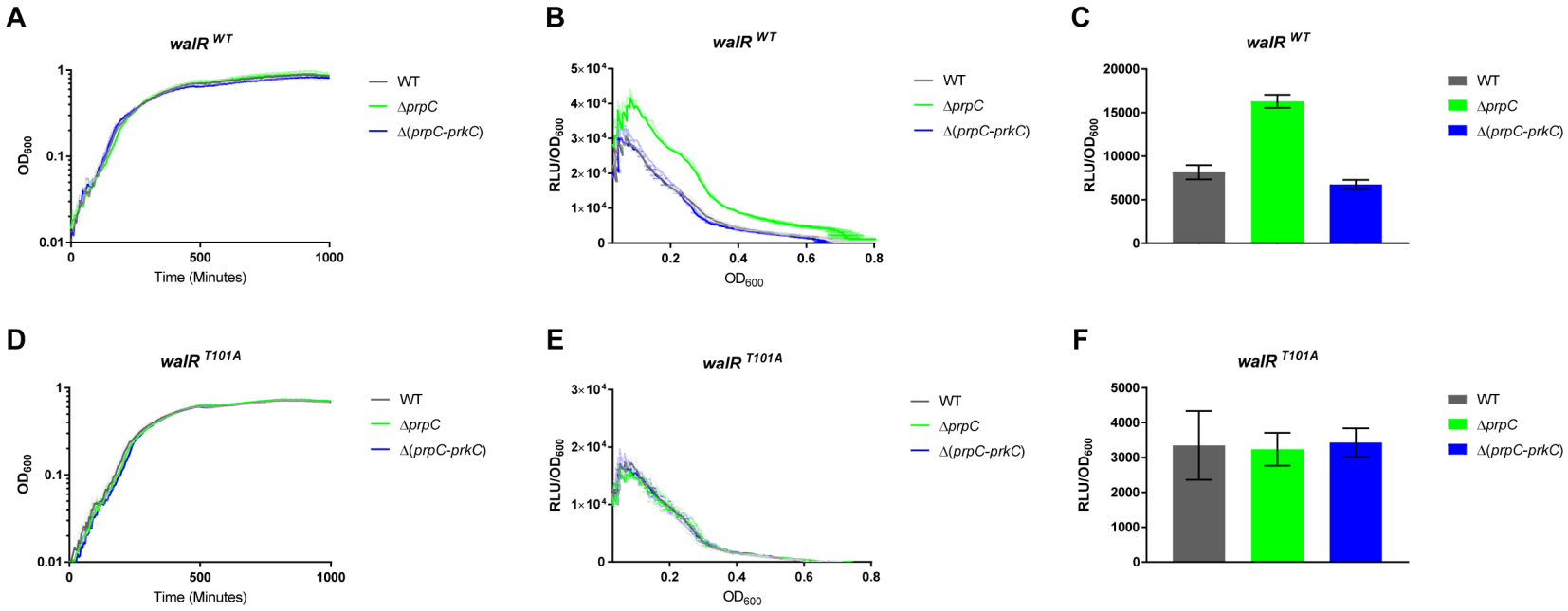

Figure S3: PrkC regulates *yocH* during log phase growth in minimal media.

A) Growth curves of P_{yocH}-*luxABCDE* in WT (gray), Δ*prpC* (green), and Δ(*prpC-prkC*) (dark blue) in an otherwise wild type background in the chemically defined minimal medium S7-glucose. Time indicates minutes post OD_{600} ~0.01 for each genotype. For all graphs solid lines indicate the means of 3 experimental replicates, and the shading indicates the standard deviation.

B) Relative luminescence units (RLU) / OD_{600} as a function of OD_{600} for the experiment shown in **A**. Throughout log phase, the normalized reporter activity in the Δ*prpC* background is significantly higher than WT or a Δ(*prpC-prkC*) background.

C) Detail of relative P_{yocH}-*luxABCDE* reporter activity (RLU/OD_{600}) at OD_{600}~0.3.

D-F) A similar experiment to **A-C** was performed in a *walR T101A* background.

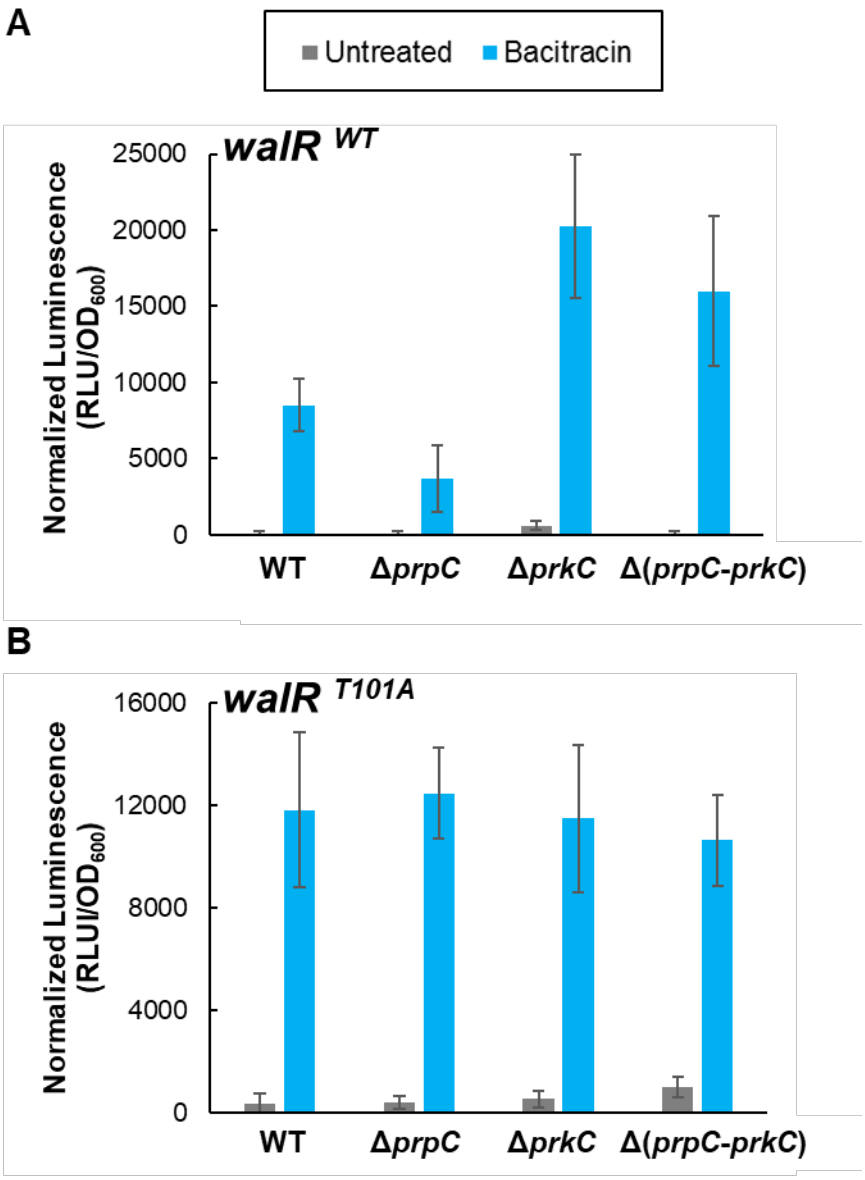

Figure S4: The Ser/Thr kinase PrkC regulates average *sasA* induction through WalR T101~P.

A) The Ser/Thr kinase PrkC and its partner phosphatase PrpC regulate *sasA* under inducing conditions. In the absence of induction, *sasA* expression is very low (gray). Bacitracin (blue) induces *sasA* expression amplifying relative changes. The average induction of *sasA* without (gray) and with bacitracin treatment (blue) was measured in otherwise WT, Δ*prpC*, Δ*prkC*, or Δ(*prpC-prkC*) backgrounds using a P_{sasA}-

177 *lux* reporter. A >4 fold change is observed between the Δ*prpC* and Δ(*prpC-prkC*)
178 backgrounds, indicating that PrkC activity represses *sasA*. Bars and lines indicate the
179 mean and standard deviation, respectively, of at least 3 biological replicates.

180 **B)** PrkC-dependent *sasA* regulation is abrogated in a non-phosphorylatable *walR T101A*
181 mutant background. The average relative induction of *sasA* without (gray) and with
182 bacitracin treatment (blue) was measured as in (**A**), but in a *walR T101A* mutant
183 background. No significant difference between genetic backgrounds is observed.

184

185

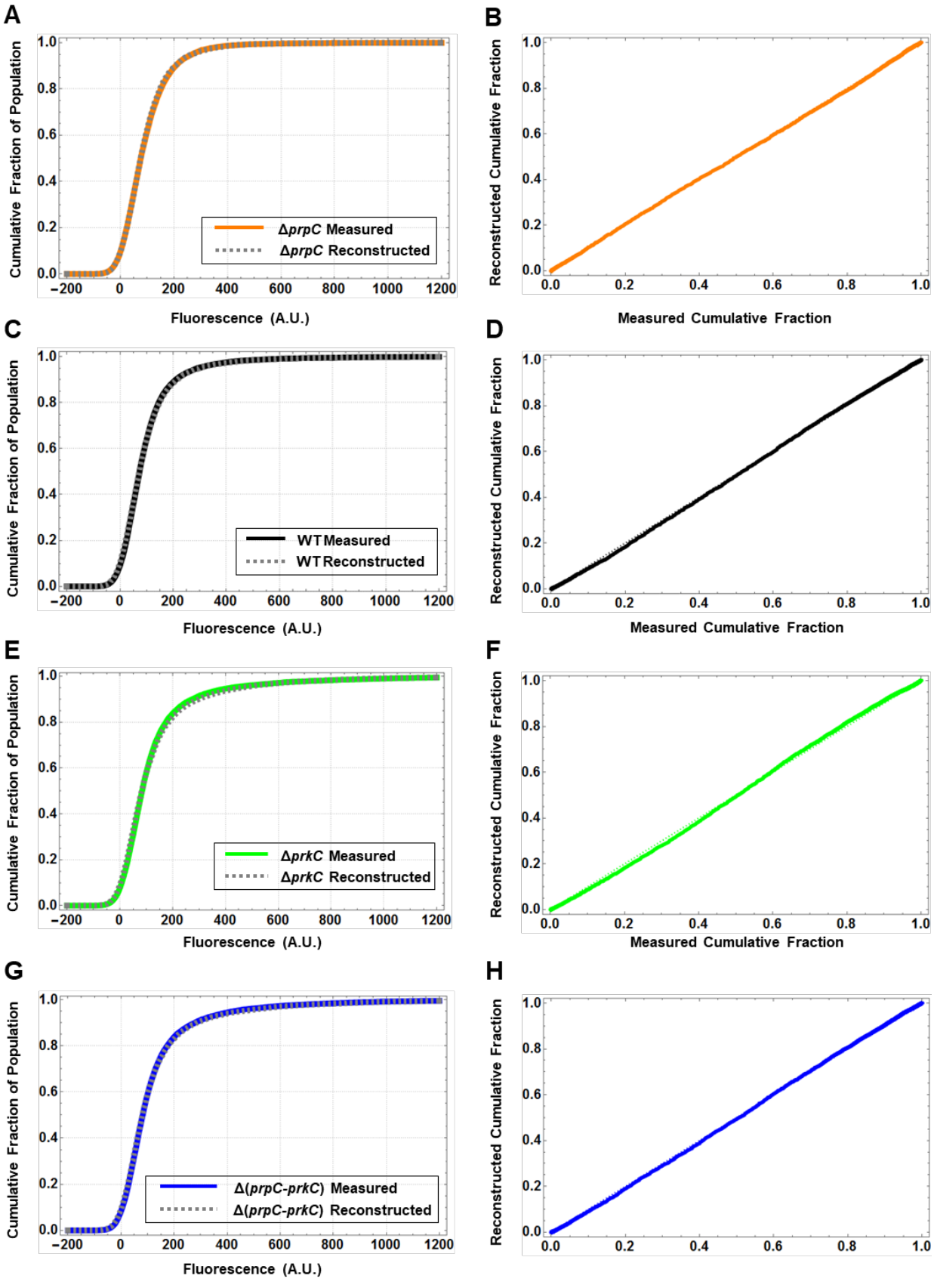
A
Cumulative Fraction of Population
Fluorescence (A.U.)
ΔprpC Measured
ΔprpC Reconstructed
B
Reconstructed Cumulative Fraction
Measured Cumulative Fraction
C
Cumulative Fraction of Population
Fluorescence (A.U.)
WT Measured
WT Reconstructed
D
Reconstructed Cumulative Fraction
Measured Cumulative Fraction
E
Cumulative Fraction of Population
Fluorescence (A.U.)
ΔprkC Measured
ΔprkC Reconstructed
F
Reconstructed Cumulative Fraction
Measured Cumulative Fraction
G
Cumulative Fraction of Population
Fluorescence (A.U.)
Δ(prpC-prkC) Measured
Δ(prpC-prkC) Reconstructed
H
Reconstructed Cumulative Fraction

186

Figure S5: Validation of the autofluorescence deconvolution method used in Figure 2.

Comparison of the measured fluorescence distributions from Fig. 2B and reconstructed distributions based on the deconvolution algorithm (main text, methods). Plots of the cumulative distribution functions of the measured data sets (solid lines) and the data set numerically reconstructed (dashed lines) using the deconvolved data and the measured autofluorescence. This was repeated for each genotype **(A)** Δ*prpC*, **(C)** WT, **(E)** Δ*prkC*, **(G)** Δ(*prpC-prkC*). To assess the agreement between the measured and reconstructed data sets for each, P-P plots were also used. For each data set the measured cumulative fraction was plotted against the reconstructed cumulative fraction (solid). A line with a slope of 1 (dashed), indicates perfect agreement. This process was repeated for **(B)** Δ*prpC*, **(D)** WT, **(F)** Δ*prkC*, and **(H)** Δ(*prpC-prkC*), and the presence of only very small deviations indicates very good agreement between the reconstructed and measured data sets.

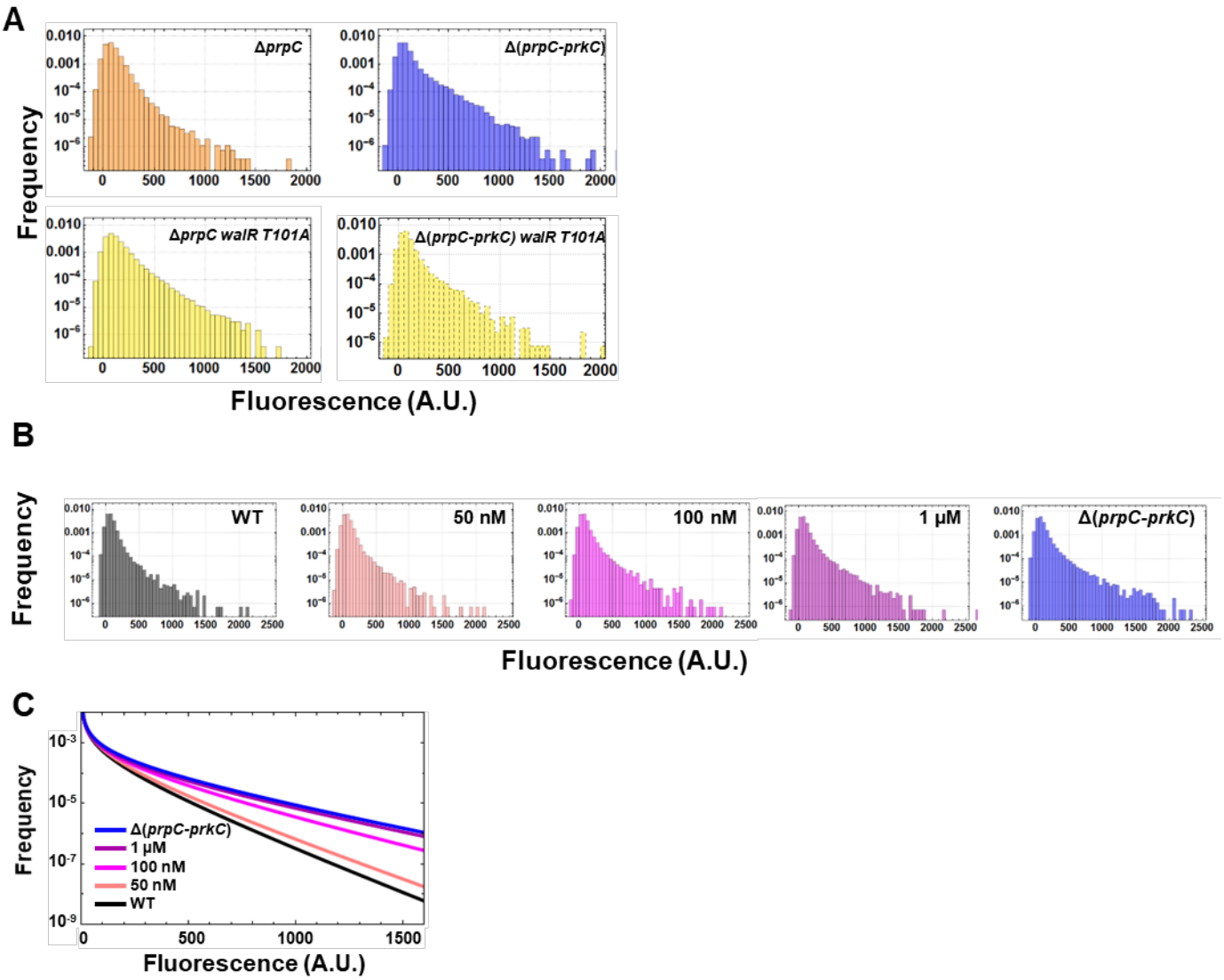

Figure S6: Additional data sets used to generate Figure 3.

A) Histograms of measured data used to generate Figure 3C. P_{sasA}-*yfp* reporter activity was quantified by flow cytometry in a Δ*prpC walR T101A* (yellow, solid) background and compared to Δ*prpC* (orange), Δ(*prpC-prkC*) (blue), and Δ(*prpC-prkC*) *walR T101A* (yellow, dashed) backgrounds in the same experiment. Each data set was obtained from ~6.0*10^4 events.

B) Histograms of measured data used to generate Figure 3D. The effect of staurosporine on *sasA* expression is dose-dependent. P_{sasA}-*yfp* reporter activity was quantified by flow cytometry during treatment with increasing concentrations of staurosporine: 0 (solvent only; black), 50, 100 nM, and 1 µM (shades of magenta), in otherwise WT populations. For reference, the distribution of P_{sasA}-*yfp* in a Δ(*prpC-prkC*) (blue) population treated with solvent only was also measured in the same experiment. Each distribution was measured from data on ~$3.0*10^4$ events.

C) Functional fits of autofluorescence-free distributions of *sasA* expression with increasing concentrations of staurosporine. A deconvolution algorithm was used to remove the contribution of autofluorescence from the measured distributions of *sasA* expression shown in **B**.

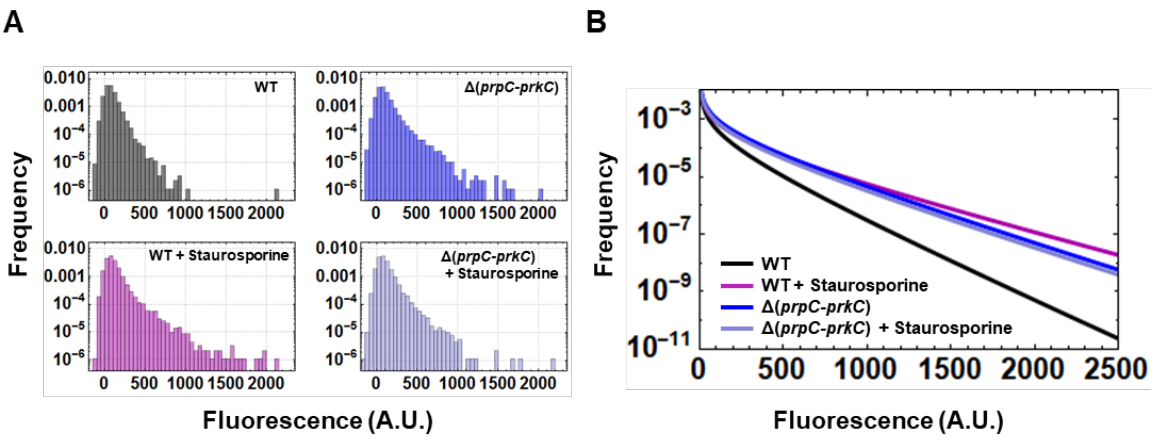

Figure S7: Additional controls for the PrkC inhibition experiment shown in Fig 3.

A) The effect of staurosporine on *sasA* requires the PrkC/PrpC system. Treatment with the kinase inhibitor staurosporine results in a PrkC-dependent increase in the frequency of cells with elevated *sasA* expression. P_{sasA}-*yfp* reporter activity was quantified by flow cytometry in WT (black) or Δ(*prpC-prkC*) (blue) untreated populations, and WT (magenta) and Δ(*prpC-prkC*) (light blue) treated populations treated with 1 μM staurosporine. Each distribution was measured from data on ~$3.0*10^4$ events.

B) Deconvolution of data shown in A from cellular autofluorescence.

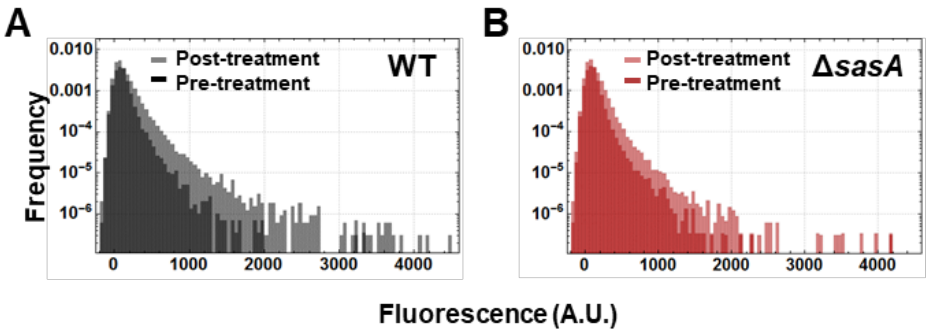

Figure S8: Distributions of *sasA* expression pre- and post-ciprofloxacin treatment used to generate the fits and model in Fig. 4.

A) Antibiotic treatment results in an increase in the number of cells with elevated *sasA* expression. Distributions of P_{sasA}-*yfp* expression in an otherwise wild type background before (dark gray) and after (light gray) ciprofloxacin treatment. Data represents ~10^5 events for each population.

B) Histograms of the distributions of P_{sasA}-*yfp* expression in a Δ*sasA* background before (dark red) and after (light red) ciprofloxacin treatment in a parallel experiment to **A**.

Table S1. Strains in figures

Figure	Panel	Strains
1	A	ELB115
	B, C, D	ELB344
2	B	ELB115, ELB116, ELB117, ELB330
	C,D	ELB115, ELB116, ELB330, ELB371,ELB369B, ELB373
3	A,B	ELB115, ELB116, ELB117, ELB330
	C	ELB330, ELB116, ELB369B, ELB373
	D	ELB115, ELB330
4	A	ELB336, ELB340
	B	ELB115
	C	ELB331
	D,E,F	ELB115, ELB331
S1	B,C	ELB499, ELB450
S2	B,C,D	ELB348
S3	A,B,C	ELB205, ELB211, ELB217
	D,E,F	ELB243, ELB299, ELB249
S4	A	ELB80, ELB81, ELB82, ELB367
	B	ELB359, ELB360, ELB362, ELB374
S5	A,B	ELB116
	C,D	ELB115
	E,F	ELB117
	G,H	ELB330
S6	A	ELB330, ELB116, ELB369B, ELB373
	B,C	ELB115, ELB330
S7	A,B	ELB115, ELB330
S8	A	ELB115
	B	ELB331

247 **Table S2: Strains Used in this Study**

Strain	Genotype	Construction	Source
***B. subtilis* strains**			
168 *trpC2* (PB2)	168 *trpC2* (WT)		Lab stock & (9)
PB702	PB2 Δ*prpC*		"
PB705	PB2 Δ*prkC*		"
PB722	PB2 Δ(*prpC-prkC*)		"
EB1385	P_{sasA}-*luxABCDE mls bla* (Note *ywaC* has been renamed *sasA*.)		(10)
ELB80	P_{sasA}-*luxABCDE mls bla*	Transformation of EB1385 into PB2.	This study
ELB81	Δ*prpC* P_{sasA}-*luxABCDE mls bla*	Transformation of EB1385 into PB702.	"
ELB82	Δ*prkC* P_{sasA}-*luxABCDE mls bla*	Transformation of EB1385 into PB705.	"
ELB113	*sacA*::P_{sasA}-*yfp cm*	Integration of pEL81 into PB2.	"
ELB115	*sacA*::P_{sasA}-*yfp cm*	Transformation of ELB113 into PB2.	"
ELB116	Δ*prpC sacA*::P_{sasA}-*yfp cm*	Transformation of ELB113 into PB702	"
ELB117	Δ*prkC* sacA::P_{sasA}-*yfp cm*	Transformation of ELB113 into PB705.	"
ELB166	Δ*sasA*::*tet*	Integration of pEL98 into PB2.	"
ELB205	*sacA*::P_{yocH}-*luxABCDE*		(6)
ELB211	Δ*prpC sacA*::P_{yocH}-*luxABCDE cm*		"
ELB217	Δ(*prpC-prkC*) *sacA*::P_{yocH}-*luxABCDE cm*		"
ELB243	*sacA*::P_{yocH}-*luxABCDE cm*, *purA-kan-walRT101A*		"
ELB249	Δ(*prpC-prkC*) *sacA*::P_{yocH}-*luxABCDE cm*, *purA-kan-walRT101A*		"
ELB299	Δ*prpC sacA*::P_{yocH}-*luxABCDE cm*, *purA-kan-walRT101A*		"
ELB330	Δ(*prpC-prkC*) *sacA*::P_{sasA}-*yfp cm*	Transformation of ELB113 into PB722.	This study
ELB331	Δ*sasA*::*tet sacA*::P_{sasA}-*yfp cm*	Transformation of ELB166 into ELB115.	"
ELB332	*amyE*::P_{ilvA}-*mcherry spec*	Integration of pEL152 into PB2.	"
ELB336	*sacA*::P_{sasA}-*yfp cm amyE*:: P_{ilvA}-*mcherry spec*	Transformation of ELB332 into ELB115.	"
ELB340	*sacA*::P_{sasA}-*yfp cm amyE*::P_{ilvA}-*mcherry spec* Δ*sasA*::*tet*	Transformation of ELB332 into ELB331.	"

ELB344	*sacA*::P_{sasA}-*yfp cm amyE*::P_{sasA}-*mcherry spec*	Integration of pEL157 into ELB115.	“
ELB345	*amyE*::P_{sigM}-*mcherry spec*	Integration of pEL158 into PB2.	“
ELB346	*sacA*::P_{sigM}-*yfp cm*	Integration of pEL159 into PB2.	“
ELB348	*sacA*::P_{sasA}-*yfp cm amyE*::P_{sigM}-*mcherry spec*	Transformation of ELB345 into ELB115.	“
ELB349	*sacA*::P_{sigM}-*yfp cm*	Transformation of ELB346 into PB2	“
ELB350	Δ*prpC sacA*::P_{sigM}-*yfp cm*	Transformation of ELB346 into PB702.	“
ELB351	Δ(*prpC-prkC*) *sacA*::P_{sigM}-*yfp cm*	Transformation of ELB346 into PB722.	“
ELB356	*purA-aph-term-tRNAs-walR T101A*	Direct transformation of Gibson assembled product *purA-aph-term-tRNAs-walR T101A*. into PB2. See below for details.	“
ELB358	*purA-aph-term-tRNAs-walR T101A*	Transformation of ELB356 into PB2.	“
ELB359	P_{sasA}-*luxABCDE mls bla purA-aph-term-tRNAs-walR T101A*	Transformation of ELB358 into ELB80.	“
ELB360	Δ*prpC* P_{sasA}-*luxABCDE mls bla purA-aph-term-tRNAs-walR T101A*	Transformation of ELB358 into ELB81.	“
ELB362	Δ*prkC* P_{sasA}-*luxABCDE mls bla purA-aph-term-tRNAs-walR T101A*	Transformation of ELB358 into ELB82.	“
ELB367	Δ(*prpC-prkC*) P_{sasA}-*luxABCDE mls bla*	Transformation of EB1385 into PB722.	“
ELB369B	Δ*prpC sacA*::P_{sasA}-*yfp* cm *purA-aph-term-tRNAs-walR T101A*	Transformation of ELB358 into ELB116.	“
ELB371	*sacA*::P_{sasA}-*yfp cm purA-aph-term-tRNAs-walR T101A*	Transformation of ELB358 into ELB115.	“
ELB373	Δ(*prpC-prkC*) *sacA*::P_{sasA}-*yfp cm purA-aph-term-tRNAs-walR T101A*	Transformation of ELB369B into ELB330.	“
ELB374	Δ(*prpC-prkC*) P_{sasA}-*luxABCDE mls bla purA-aph-term-tRNAs-walR T101A*	Transformation of ELB358 into ELB367.	“
IP386	*amyE*::P_{veg}-*mcherry spec*	Integration of pIP384 into PB2.	“
ELB499	*sacA*::P_{sasA}-*yfp cm amyE*::P_{veg}-*mcherry spec*	Transformation of IP386 into ELB115.	“
ELB450	Δ*sasA*::*tet sacA*::P_{sasA}-*yfp cm amyE*::P_{veg}-*mcherry spec*	Transformation of IP386 into ELB331.	“

Construction of ELB356:

The Gibson assembled product *purA-aph-term-tRNAs-walR T101A* was created in two steps. In the first step, the *aph-term* encoding kanamycin resistance and a terminator was introduced

using Gibson assembly to create: '*purA-aph-term-tRNAs-walR-walK'* using the primers GA-purA-u1, GA-purA-l1, GA-aph-u1, GA-aph-l1, GA-termwalR-u1, GA-termwalR-l1 to amplify the chromosomal homology and pDG780 as the template for *aph*. Then a product containing the '*purA-aph-term-tRNAs-walR T101A-walK'* was created by soeing PCR using: purA-PCR-u2, walR-T101A-l1, walR-T101A-u1, walK-PCR-l1 using the product of the first step as a template.

Table S3: Plasmids Used in this Study

Plasmid			
Stock Vectors			
pECE174-YFP			(11)
pDG780			(12)
pAF095			Lab Stock
pAF328			Lab Stock
pSac-cm			(13)
Vector	**Genotype**	**Construction**	**Source**
pEL81	pSac-cm P_{sasA}-*yfp*	P_{sasA}-*yfp* transcriptional reporter in pSac-cm. Made by amplifying the *sasA* promoter using EcoRI-PywaC-u1 and BamHI-PywaC-l1. The resulting product was digested with EcoRI/BamHI and ligated to pECE174-YFP digested with same.	This study
pEL98	pDG780 *sasA*::*tet*	*sasA*::*tet* knockout vector. Made by gibson assembly into pDG780 digested with EcoRI/SalI. Primers used to assemble the inserts are: pDG780-ywaC-u1, Tet-ywaC-l1, ywaC-tet-u1, ywaC-tet-l1, Tet-ywaC-u1, pDG780-ywaC-l1. pAF095 was used as a template for *tet*.	"
pEL151	pDG1730 *rbs-mcherry spec*	RBS-*mcherry* vector for making *mcherry* transcriptional reporters for integration at *amyE*. Made by amplifying *mcherry* from pAF328 using HindIII-mCherry-u1 (introducing a new RBS) and BamHI-mCherry-l1. Digested the resulting product with BamHI/HindIII and ligated	"

		to pDG1730 digested with same.	
pEL152	pDG1730 P_{ilvA}-*mcherry spec*	P_{ilvA}-*mcherry* reporter for integration at amyE. Made by amplifying the *ilvA* promoter region using EcoRI-PilvA-u1 and HindIII-PilvA-l1. The resulting product was digested with EcoRI/HindIII and ligated to pEL151 digested with same.	"
pEL157	pDG1730 P_{sasA}-*mcherry spec*	P_{sasA}-*mcherry* reporter for integration at *amyE*. Made by amplifying the *sasA* promoter region using EcoRI-PywaC-u1 and HindIII-PywaC-l2. The resulting product was digested with EcoRI/HindIII and ligated to pEL151 cut with same.	"
pEL158	pDG1730 P_{sigM}-*mcherry*	P_{sigM}-*mcherry* reporter for integration at *amyE*. Made by amplifying the *sigM* promoter using EcoRI-PsigM-u1 and HindIII-PsigM-l1. Digested the product with EcoRI/HindIII and ligated to pEL151 digested with same.	"
pEL159	pSac-cm P_{sigM}-*yfp*	P_{sigM}-*yfp* reporter for integration at *sacA*. Made by amplifying the *sigM* promoter using EcoRI-PsigM-u1 and BamHI-PsigM-l1. Digested the product with EcoRI/BamHI and ligated to pECE174-YFP digested with same.	"
pIP384	pDG1730 P_{veg}-*mcherry spec*	P_{veg}-*mcherry* reporter for integration at *amyE*. Made by phosphorylating	"

		and annealing primers encoding the *veg* promoter: IP_P_1130 and IP_P_1131. Digested the product with EcoRI/HindIII and ligated to pEL151 digested with same.	

261

262

263 **Table S4: Oligos used in this study**

Name	Sequence (5'-3')
EcoRI-PywaC-u1	GGCTAGAATTCGTCCAGAACGAAATGCCGATG
BamHI-PywaC-l1	GGCTAGGATCCCGGAACTTTATCCGCTGTCC
pDG780-ywaC-u1	TTGGGTACCGGGCCCCCCCTCGAGGTCGACATTCAGACAGATAAGATCAATATG
Tet-ywaC-l1	ACAATATGGCCCGCTTTAACGGAACTTTATCCG
ywaC-tet-u1	AGTTCCGTTAAAGCGGGCCATATTGTTGTATAAG
ywaC-tet-l1	TTTCTCATCTAGGGAACTCTCTCCCAAAGTTG
Tet-ywaC-u1	TGGGAGAGAGTTCCCTAGATGAGAAAATGCTGG
pDG780-ywaC-l1	ACTAGTGGATCCCCCGGGCTGCAGGAATTCGTGAACTTCAACTTAGATATGGTAG
HindIII-mCherry-u1	GGTCAAAGCTTAAAGGAGGAAAGTCACATTATGGTTTCCAAGGGCGAGG
BamHI-mCherry-l1	GGTCAGGATCCTTATTTGTACAGCTCATCC
EcoRI-PilvA-u1	GGTCAGAATTCGGTGCACTATTCATCAATTGGC
HindIII-PilvA-l1	GGTCAAAGCTTGTTTTAAATCCCTATTTAATATG
HindIII-PywaC-l2	GGTCAAAGCTTCGGAACTTTATCCGCTGTCC
EcoRI-PsigM-u1	GGCTAGAATTCCACTATCTTTTCCCCTCTGG
HindIII-PsigM-l1	GGTCAAAGCTTCTATGTTATACACGCATAAG
BamHI-PsigM-l1	GGCTAGGATCCCTATGTTATACACGCATAAG
IP_P_1130	AGCTCATTTATTGTACAACACGAGCCCATTTTTGTCAAATAAAATTTAAATTATATC AACGTTAATAAGG
IP_P_1131	AATTCCTTATTAACGTTGATATAATTTAAATTTTATTTGACAAAAATGGGCTCGTGT TGTACAATAAATG

264

265

References

1. Wang JD, Sanders GM, & Grossman AD (2007) Nutritional control of elongation of DNA replication by (p)ppGpp. *Cell* 128(5):865-875.
2. Vasantha N & Freese E (1980) Enzyme changes during Bacillus subtilis sporulation caused by deprivation of guanine nucleotides. *J Bacteriol* 144(3):1119-1125.
3. Harwood CR & Cutting SM eds (1990) *Molecular biological methods for Bacillus* (Wiley, New York).
4. Schindelin J*, et al.* (2012) Fiji: an open-source platform for biological-image analysis. *Nat Methods* 9(7):676-682.
5. Miyashiro T & Goulian M (2007) Single-cell analysis of gene expression by fluorescence microscopy. *Methods Enzymol* 423:458-475.
6. Libby EA, Goss LA, & Dworkin J (2015) The Eukaryotic-Like Ser/Thr Kinase PrkC Regulates the Essential WalRK Two-Component System in Bacillus subtilis. *PLoS Genet* 11(6):e1005275.
7. Corsetti JP*, et al.* (1988) Correction of cellular autofluorescence in flow cytometry by mathematical modeling of cellular fluorescence. *Cytometry* 9(6):539-547.
8. Taniguchi Y*, et al.* (2010) Quantifying E. coli proteome and transcriptome with single-molecule sensitivity in single cells. *Science* 329(5991):533-538.
9. Gaidenko TA, Kim TJ, & Price CW (2002) The PrpC serine-threonine phosphatase and PrkC kinase have opposing physiological roles in stationary-phase Bacillus subtilis cells. *J Bacteriol* 184(22):6109-6114.
10. D'Elia MA*, et al.* (2009) Probing teichoic acid genetics with bioactive molecules reveals new interactions among diverse processes in bacterial cell wall biogenesis. *Chemistry & biology* 16(5):548-556.
11. Eldar A*, et al.* (2009) Partial penetrance facilitates developmental evolution in bacteria. *Nature* 460(7254):510-514.
12. Guerout-Fleury AM, Shazand K, Frandsen N, & Stragier P (1995) Antibiotic-resistance cassettes for Bacillus subtilis. *Gene* 167(1-2):335-336.
13. Middleton R & Hofmeister A (2004) New shuttle vectors for ectopic insertion of genes into Bacillus subtilis. *Plasmid* 51(3):238-245.